

Damping characteristics of three-layer beam-damper under harmonic loading

Zhuk Y. A.

*Taras Shevchenko National University of Kyiv
64 Volodymyrska str., 01601, Kyiv, Ukraine*

(Received 1 April 2014)

Thermomechanical behavior of inhomogeneous viscoplastic structures under cyclic loading is investigated for the problem of harmonic bending and dissipative heating of a three layer beam. Two problem statements are used. One is based on the generalized thermomechanically consistent flow theory (complete problem statement) and the other one is the approximate scleronomic model implementation (approximate problem statement). Aluminium alloy and steel are chosen as the materials of layers. Comparison of the results obtained for complete and approximate problem statements is performed. Comparative estimation of beam loss coefficients for different configurations is also performed.

Keywords: *thermomechanical coupling, beam-damper, loss coefficient*

2000 MSC: 74, 74F, 74C, 74F05

UDC: 539.3

1. Introduction

The forced-vibration analysis of structures and their elements occupies an important place in the mechanics of deformable systems. This research area attracts great interest because of the need of deeper theoretical analysis (especially of nonlinear systems) and purely practical requirements in various fields of engineering. Under intensive loading, there are several factors that determine the behavior of multilayer structures. Among them are nonlinearity of material properties, the heterogeneity of the stress-strain state (which is due to the layered structure), and the coupling of the mechanical and thermal fields. In particular, intensive loading may cause plastic deformation of elements of damping systems [1,2], building structures [3,4], test specimens in low-cycle fatigue tests [5,6], etc. This may result in elevated temperatures due to dissipative heating. In turn, the heating may change the strength characteristics of the structure, deteriorate its performance, and, under adverse conditions, even cause the failure. The heterogeneity of the stress-strain state is an additional complicating factor of the problem [7,8].

The present work is devoted to investigation of energy absorption and dissipation aspects of the problem considered for multi-layer structures. The main aim is to determine the part of energy that can be safely absorbed/dissipated by a three layer beam. One of the basic issues for such investigation is determination of energy dissipation characteristics. The usual procedure lies in obtaining such energy quantities as stored and dissipated energies and loss coefficient for the case of cyclic loading.

Amount of structural members subjected to cyclic loading is vast. There are different technological objects, elements of power equipment, dampers etc. [1,2] among these structural elements. Some of them can deform inelastically [9]. It can cause significant heating due to the internal dissipation of mechanical energy and changing of functional characteristics of elements under long term cyclic loading. Investigation of this class of objects and processes demands the implementation of material models that take into account properly both mechanical and thermal aspects of member state. On the author's opinion, generalized flow theories are most promising from this point of view. Within the framework of these theories, thermodynamics of irreversible processes is used to derive the correct

system of constitutive equations and heat conduction equation (see, for example, [10–14]). The refined thermodynamically consistent model of coupled thermo-viscoplastic material behavior was elaborated on the base of Bodner-Partom model in the works [11,15,16]. This model describes isotropic and anisotropic hardening by means of one scalar and one tensor internal variables.

For the particular case of cyclic (harmonic) loading, the approximate scleronomic model of coupled thermomechanical behavior of elastic-viscoplastic bodies was elaborated in papers [15–18]. This model was formulated in terms of amplitudes of mechanical field variables, averaged over the period temperature and complex mechanical moduli (see also [19,20]). In the present paper original “complete” and approximate models are applied to investigate coupled thermomechanical behavior of structurally inhomogeneous viscoplastic bodies under harmonic loading. Quasi-static vibration and dissipative heating of a three layer beam subjected to harmonic bending are under consideration. Set of mechanical field variables and heating temperatures obtained as a result of implementation of both model are compared. Some aspects of storage and dissipation of energy under cyclic bending, that have particular interest for vibration damping, are investigated as well.

2. Problem statement

The problem of vibration and heat dissipation of a three layer viscoplastic beam $|x| \leq a$, $|y| \leq b$ under kinematic harmonic bending applied on its ends is studied for the plane stress state (Fig. 1). It is assumed that the inner and outer layers are fabricated from different viscoplastic materials. Ideal thermal and mechanical contact is assumed on the boundaries between layers. In accordance with [15,16,18] the problem statement consists of Cauchy’s relations

$$\varepsilon = \frac{1}{2} [\nabla \mathbf{u} + (\nabla \mathbf{u})^T], \quad (1)$$

equation of quasi-static equilibrium (2), energy balance equation (3), constitutive equations of material behavior, initial and thermomechanical conditions on the outer boundary (4)–(6)

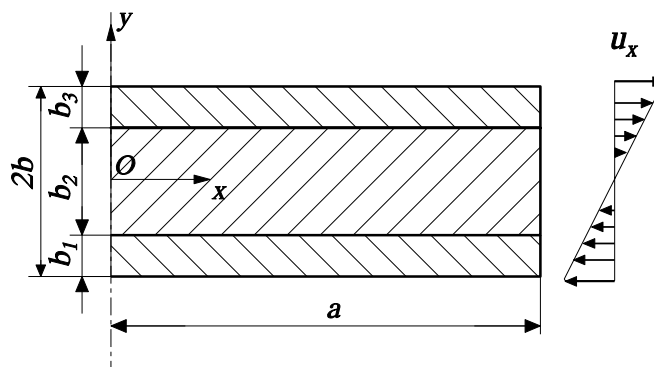


Fig. 1. Three layer beam-damper lay-up.

$$\nabla \cdot \boldsymbol{\sigma} = 0 \quad \text{in } V, \quad (2)$$

$$c_V \dot{\theta} + 3\alpha\theta K_V (\text{tr } \dot{\boldsymbol{\varepsilon}} - 3\alpha\dot{\theta}) - D' - k\Delta\theta = r, \quad (3)$$

$$\theta(0) = \theta_0, \quad (4)$$

$$u_x = \pm \hat{\varepsilon} y \sin \omega t, \quad \sigma_{xy} = 0, \quad |x| = a; \quad \sigma_{yy} = \sigma_{xy} = 0, \quad |y| = b, \quad (5)$$

$$-k\nabla\theta = \gamma(\theta - \theta_0), \quad |x| = a, \quad |y| = b. \quad (6)$$

It is assumed that viscoplastic behavior of materials is described by the Bodner-Partom's model (see, for example [11,12]). Generalization and thermodynamic analysis of it were performed by Senchenkov and Zhuk [15] and Senchenkov, Zhuk et al. [16]. It was accepted for this model that total strain is a sum of elastic, inelastic and thermal parts

$$\boldsymbol{\varepsilon} = \boldsymbol{\varepsilon}^e + \boldsymbol{\varepsilon}^p + \boldsymbol{\varepsilon}^\theta, \quad (7)$$

$$\boldsymbol{\varepsilon}^\theta = \mathbf{I} \int_{\theta_0}^{\theta} \alpha(\theta') d\theta'. \quad (8)$$

The model also incorporates the Hooke's law for elastic strain (9), the flow law (10) and the evolution equation for parameters of isotropic and anisotropic hardening (11), (12)

$$\mathbf{s} = 2G(\mathbf{e} - \boldsymbol{\varepsilon}^p), \quad \text{tr } \boldsymbol{\sigma} = 3K_V \text{tr}(\boldsymbol{\varepsilon} - \boldsymbol{\varepsilon}^\theta), \quad (9)$$

$$\dot{\boldsymbol{\varepsilon}}^p = \frac{D_0}{\sqrt{J_2}} \exp\left[-\frac{1}{2}\left(\frac{Z^2}{3J_2}\right)^n\right] \mathbf{s}; \quad Z = K + D, \quad (10)$$

$$\dot{K} = m_1(K_1 - K)\dot{W}_p - A_K K_1 \left(\frac{K - K_2}{K_1}\right)^{r_K}, \quad (11)$$

$$\dot{\boldsymbol{\beta}} = m_2(D_1 \mathbf{u} - \boldsymbol{\beta})\dot{W}_p - A_D K_1 \left[\frac{(\boldsymbol{\beta} : \boldsymbol{\beta})^{1/2}}{K_1}\right]^{r_D} \mathbf{V} \quad (12)$$

where

$$J_2 = \mathbf{s} : \mathbf{s}/2, \quad \dot{W}^p = \boldsymbol{\sigma} : \dot{\boldsymbol{\varepsilon}}^p, \quad \mathbf{u} = \mathbf{s}/(\mathbf{s} : \mathbf{s})^{1/2}, \\ \mathbf{V} = \boldsymbol{\beta}/(\boldsymbol{\beta} : \boldsymbol{\beta})^{1/2}, \quad D = \boldsymbol{\beta} : \mathbf{u}.$$

The following notations were used in Eqns (1)–(12): \mathbf{u} is the displacement vector; $\boldsymbol{\varepsilon}$ and $\boldsymbol{\sigma}$ are the tensors of total strain and stress; $\boldsymbol{\varepsilon}^e$, $\boldsymbol{\varepsilon}^p$ and $\boldsymbol{\varepsilon}^\theta$ are the elastic, inelastic and thermal components of strain tensor respectively; \mathbf{e} and \mathbf{s} are the deviators of strain and stress tensors; K and $\boldsymbol{\beta}$ are the parameters of isotropic and anisotropic hardening correspondingly; θ is the temperature; G and K_V are the shear and bulk moduli respectively; D' is the rate of energy dissipation; k is the heat conductivity coefficient; c_V is the specific heat capacity for constant volume; α is the thermal expansion coefficient; r is the power of thermal sources; γ is the heat transfer coefficient; θ_0 is the temperature of environment. The constants D_0 , D_1 , K_0 , K_1 , K_2 , m_1 , m_2 , A_K , A_D , r_K , r_D and n are the model parameters. In accordance with the model formulation, coefficients D_0 , D_1 , K_1 , m_1 , m_2 , r_K and r_D are temperature independent while K_0 , K_2 , A_K , A_D , K_V and G that depend on temperature. In Eqns (1)–(12) \mathbf{I} denotes the unit tensor of appropriate rank; $\mathbf{a} : \mathbf{b}$ is a convolution of tensors \mathbf{a} and \mathbf{b} ; $\text{tr } \mathbf{a}$ is a trace of the tensor \mathbf{a} ; $(\dot{\cdot}) = \partial(\cdot)/\partial t$ and Δ is Laplacian operator.

Numerical integration of problem (1)–(12) is significantly complicated by the necessity of taking into account the total prehistory of deformation in the case of multiple cycle loading.

3. Thermodynamic analysis of model

The formulation of the coupled thermo-viscoplasticity problem demands the model of material behaviour to be consistent with thermodynamics of irreversible processes. In this section the thermodynamic analysis of the Bodner-Partom model will be performed.

The Helmholtz energy ψ is taken as a thermodynamic potential

$$\psi = U - \eta\theta, \quad \psi = \psi(\varepsilon, \theta, \alpha_k) \quad (13)$$

where U is the internal energy; η is the entropy; α_k is the set of internal variables.

The energy equation takes the form

$$\dot{U} - \boldsymbol{\sigma} : \dot{\boldsymbol{\varepsilon}} + \operatorname{div} \mathbf{h} = r \quad (14)$$

where \mathbf{h} is the heat flux.

Taking into account Eqn (14), the second law of thermodynamics in Planck form reduces to the dissipative inequality

$$\boldsymbol{\sigma} : \dot{\boldsymbol{\varepsilon}} = \dot{\psi} - \eta\dot{\theta} \geq 0. \quad (15)$$

Employing the standard thermodynamic procedure, the defining equations may be established on the base of Eqns (14) and (15), taking into account Eqn (8)

$$\boldsymbol{\sigma} = \frac{\partial \psi}{\partial \boldsymbol{\varepsilon}}, \quad \eta = -\frac{\partial \psi}{\partial \theta}, \quad A_k = \frac{\partial \psi}{\partial \alpha_k}, \quad k = \overline{1, N}. \quad (16)$$

Here, A_k are the thermodynamic forces conjugated with the variables (thermodynamic displacements) α_k . The dissipative inequality then takes the form

$$\boldsymbol{\sigma} : \dot{\boldsymbol{\varepsilon}}^p - A_k \dot{\alpha}_k = D' \geq 0, \quad (17)$$

According to Eqn (17), D' is the difference between the plastic power and the rate of variation of hidden stored energy \dot{W}_s

$$\dot{W}_s = A_k \dot{\alpha}_k. \quad (18)$$

It follows from Eqn (17) that only a part of the plastic work is converted into heat. The portion of it that is phenomenologically related to hardening is stored in the material. This energy is associated with the additional stored energy due to the dislocation kinetics and also with the changes in the surface energy of the pores.

The following evolution equations for the internal variables should be added to Eqn (16)

$$\dot{\alpha}_k = \bar{\alpha}_k(\varepsilon, \theta, \alpha_j), \quad k, j = \overline{1, N}. \quad (19)$$

Let us assume that the body occupies the region V bounded by surface S with the external normal \mathbf{n} . Taking account of Eqns (13), (16) and (17), Eqn (14) transforms into

$$\theta \dot{\eta} = \operatorname{div} \mathbf{h} + D' + r, \quad \text{in } V. \quad (20)$$

In order to obtain the Bodner-Partom model from the general model, we determine the appropriate form of Eqn (13) and (19). In the generalized models the thermodynamic forces A_k are associated with the hardening parameters. In particular, for the Bodner-Partom model A_k are equivalent to the set $\{K, \beta\}$. The conjugate internal variables are denoted by δ and α .

According to Senchenkov and Zhuk [15] and Senchenkov, Zhuk et al. [16], the following expression can be written for the free energy

$$\psi = G(\mathbf{e} - \boldsymbol{\varepsilon}^p) : (\mathbf{e} - \boldsymbol{\varepsilon}^p) + \frac{1}{2} K_V [\operatorname{tr}(\boldsymbol{\varepsilon} - \boldsymbol{\varepsilon}^p) - 3 \boldsymbol{\varepsilon}^p]^2 + \frac{m_1 K_1^2 \delta^2}{2c} + \frac{m_2 D_1^2 (\boldsymbol{\alpha} : \boldsymbol{\alpha})}{2d} - \int_{\theta_0}^{\theta} dx \int_{\theta_0}^{\theta} \frac{c_V(y)}{y} dy. \quad (21)$$

Here $c_V(\theta)$ is the isochoric specific heat; c and d are the dimensionless constants.

As it follows from Eqns (11), (12), and (19), the evolution equations for the thermodynamic forces are specified in the mechanical model, whereas the equations for thermodynamic displacements are employed in the thermodynamic analysis. Obviously, these equations must be consistent. Determining the thermodynamic forces from Eqn (16) by means of Eqn (21) and then differentiating both sides of the resulting equations with respect to the time, we find that

$$\begin{aligned}\dot{K} &= \frac{d}{dt} \left(\frac{\partial \psi}{\partial \delta} \right) = \frac{m_1 K_1^2}{c} \dot{\delta}, \\ \dot{\beta} &= \frac{d}{dt} \left(\frac{\partial \psi}{\partial \alpha} \right) = \frac{m_2 D_1^2}{d} \dot{\alpha}.\end{aligned}\quad (22)$$

It is readily evident that substitution of the evolution equations obtained by Senchenkov, Zhuk et al. [16]

$$\dot{\delta} = c(1 - K/K_1) \dot{W}_p/K_1 - cA_K K (K_1 m_1)^{-1} [(K - K_2)/K_1]^{r_K}, \quad (23)$$

$$\dot{\alpha} = d(\mathbf{u} - \beta/D_1) \dot{W}_p/D_1 - dA_D (D_1^2 m_2)^{-1} [(\beta : \beta)^{1/2}/K_1]^{r_D} \beta / (\beta : \beta)^{1/2} \quad (24)$$

into Eqn (22) yields Eqns (11) and (12). Taking into account of Eqns (17) and (23), (24), one can find the following expression for the dissipation rate

$$D' = \boldsymbol{\sigma} : \dot{\boldsymbol{\varepsilon}}_p - \beta : \dot{\boldsymbol{\alpha}} - K \dot{\delta} = \dot{W}_p - \dot{W}_s, \quad (25)$$

$$\dot{W}_s = \dot{W}_{s\beta} + \dot{W}_{sK} = \beta : \dot{\boldsymbol{\alpha}} + K \dot{\delta}. \quad (26)$$

In Eqn (26), the accumulation rate of stored energy \dot{W}_s is divided into parts associated with the anisotropic $\dot{W}_{s\beta}$ and isotropic \dot{W}_{sK} hardening.

The analysis of Eqns (11), (12), (25) and (26) shows that the coefficients c and d in Eqns (21), (23) and (24) do not appear in the equations of the mechanical model described in Sect. 2. However, they are thermodynamically significant: they determine the portion of the plastic work converted into heat.

Equation (9) for $\boldsymbol{\sigma}$ and the equation for η are found by differentiating the free energy in Eqn (21) according to Eqn (16). To eliminate cumbersome computations for the entropy, we assume that thermo-mechanical characteristics of the material and coefficients in Eqn (21) do not depend on the temperature. After simple transformations, we write Eqn (20) in the form

$$c_{V0} \dot{\theta} + 3\alpha_0 \theta K_V (\text{tr } \dot{\boldsymbol{\varepsilon}} - 3\alpha_0 \dot{\theta}) - D' - k \Delta \theta = r, \quad (27)$$

where c_{V0} and α_0 are the specific heat and linear thermal expansion coefficients respectively at the reference temperature $\theta = \theta_0$; the dissipative function D' is determined by Eqns (23)–(25).

The formulation of the coupled problem derived here is valid for arbitrary deformation processes in materials satisfying the Bodner-Partom equations.

4. Approximate scleronomic model of coupled thermomechanical behavior of viscoplastic bodies

To avoid the complication mentioned, the approximate scleronomic model was developed. It incorporates the complex characteristics concept, and was initially elaborated for the particular case of proportional harmonic loading.

It is assumed that for the harmonic excitation of material element

$$\mathbf{e}(t) = \mathbf{e}'(t) \cos \omega t - \mathbf{e}''(t) \sin \omega t,$$

the corresponding response is also close to harmonic law

$$\mathbf{s}(t) = \mathbf{s}'(t) \cos \omega t - \mathbf{s}''(t) \sin \omega t. \quad (28)$$

As a result, the complex amplitudes of total and plastic strain deviators $\tilde{\mathbf{e}} = \mathbf{e}' + i\mathbf{e}''$ and $\tilde{\mathbf{e}}^p = \mathbf{e}^{p'} + i\mathbf{e}^{p''}$ as well as the amplitude of stress deviator $\tilde{\mathbf{s}} = \mathbf{s}' + i\mathbf{s}''$ are related by means of complex shear modulus \tilde{G}_N , $\tilde{G}_N = G'_N + iG''_N$ and plasticity coefficient $\tilde{\chi}_N$, $\tilde{\chi}_N = \chi'_N - i\chi''_N$ in each cycle as follows

$$\tilde{\mathbf{s}} = 2\tilde{G}_N\tilde{\mathbf{e}}; \quad \tilde{\mathbf{e}}^p = \tilde{\chi}_N\tilde{\mathbf{e}}, \quad N = 1, 2, \dots \quad (29)$$

where \tilde{G} and $\tilde{\chi}$ are the functions of tensor of strain amplitude intensity e_0 , frequency ω and temperature θ , N is the cycle number. In the general case $\tilde{G} = \tilde{G}(e_0, \omega, \theta)$, $\tilde{\chi} = \tilde{\chi}(e_0, \omega, \theta)$, where $e_0 = \mathbf{e}' : \mathbf{e}' + \mathbf{e}'' : \mathbf{e}''$.

The imaginary parts of characteristics are determined from the condition of equality of dissipated energies over the period

$$G''_N = \langle D' \rangle_N \omega e_0^2, \quad \chi''_N = G''_N / G, \quad (30)$$

and real parts are obtained from the condition of equivalence of generalized cyclic diagrams $\sigma_{aN} = \sigma_{aN}(e_0, \omega)$ and $\varepsilon_{aN}^p = \varepsilon_{aN}^p(e_0, \omega)$, that relates amplitudes of the equivalent plastic strain ε_{aN}^p and stress σ_{aN} in the N^{th} cycle

$$G'_N(e_0, \omega) = \left[\frac{\sigma_{aN}^2(e_0, \omega)}{4e_0^2} - G''_N{}^2(e_0, \omega) \right]^{1/2}, \quad \chi'_N(e_0, \omega) = \left[\frac{\varepsilon_{aN}^{p2}(e_0, \omega)}{e_0^2} - \chi''_N{}^2(e_0, \omega) \right]^{1/2}, \quad (31)$$

where $\langle \cdot \rangle = \frac{1}{T} \int_{(N-1)T}^{NT} (\cdot) dt$, $T = \frac{2\pi}{\omega}$.

Dissipation and cyclic diagrams are calculated by means of direct numerical integration of the Bodner-Partom model equations for the case of torsion of a hollow thin-walled cylinder.

Averaging energy equation (3) over the period of vibration and neglecting thermoelastic effects one can obtain

$$c_V \langle \dot{\theta} \rangle - k \Delta \langle \theta \rangle - \langle D' \rangle_N = 0, \quad (32)$$

where $\langle \theta \rangle$ is the averaged temperature.

Averaged dissipation function is determined as

$$\langle D' \rangle_N = \langle \dot{W}_p \rangle_N.$$

The equation of quasi-static equilibrium takes the form

$$\nabla \cdot \tilde{\boldsymbol{\sigma}} = 0 \quad (33)$$

The following mechanical boundary conditions (5) and thermal boundary and initial conditions (6), (4) should be added to Eqns (29)–(33)

$$\tilde{u}_x = \mp i \hat{\varepsilon} y, \quad \tilde{\sigma}_{xy} = 0, \quad |x| = a; \quad \tilde{\sigma}_{yy} = \tilde{\sigma}_{xy} = 0, \quad |y| = b, \quad (34)$$

$$-k \nabla \langle \theta \rangle = \gamma (\langle \theta \rangle - \theta_0), \quad |x| = a, \quad |y| = b, \quad (35)$$

$$\langle \theta \rangle = \theta_0, \quad t = 0 \quad (36)$$

where $\hat{\varepsilon}$ is loading parameter.

The approximate scleronomic model of transient thermomechanical response of viscoplastic solids is given by Eqns (29)–(33). The approximate problem statement for thermomechanical behavior of viscoplastic solids consists of the equations mentioned along with the Eqns (32), (33) and conditions (34)–(36).

5. Material properties and solution technique

Aluminium alloy and steel were chosen as the materials of layers. Their mechanical properties and generalized model constants are given in Table 1. Stabilized complex moduli ($N \rightarrow \infty$) of approximate model for both materials are plotted in Fig. 2. Curves 1 and 2 show the dependence of G'/G vs strain intensity for aluminium alloy and steel respectively. Similar dependencies for G''/G are depicted by curves 3 and 4.

Table 1. Mechanical properties and generalized model constants used.

Parameter	Aluminium alloy	Steel
$\rho, \text{kg/m}^3$	2640	7820
$c_\rho, \text{J/kg}\cdot^\circ\text{K}$	921.0	485.9
$E \cdot 10^{-5}, \text{MPa}$	0.816	2.12
ν	0.34	0.30
$k, \text{W/m}\cdot^\circ\text{K}$	90.00	30.98
$\alpha \cdot 10^{-6}, 1/^\circ\text{K}$	23.0	12.0
n	2.06	1.00
D_0, s^{-1}	10^4	10^4
D_1, MPa	80	0
K_0, MPa	323.6	3145
K_1, MPa	647.4	4000
K_2, MPa	35	0
m_1, MPa^{-1}	0.182	0.300
m_2, MPa^{-1}	3.7	0.0

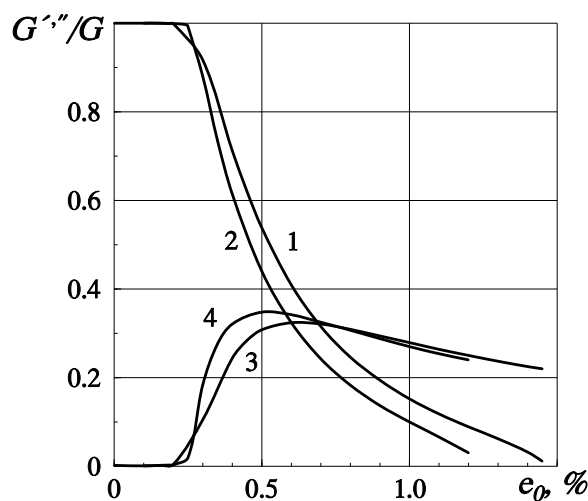


Fig. 2. Stabilized complex moduli of approximate model for aluminium alloy and steel.

The technique of numerical solution for the complete problem statement is designed as double iterative process. The first (internal) process is formed by numerical integration of evolution equations. The second iterative process is related to the quasi-static equilibrium equation and heat conduction equation integration. The implicit Euler's method is used for the integration of evolution equations. A simple integration technique is employed for solution of non-linear transcendental system of equations, which arises at each time step. The Steffensen-Eytken's technique is used to accelerate the process convergence. The initial iteration is calculated by means of square extrapolation of values from three previous time steps. The equilibrium and heat conductivity problems are solved by means of FEM. Quadrilateral eight-node elements with four Gauss points are used. The plastic strain is incorporated into fictive mass forces and is not varied under variation procedure. Time step correction technique is applied. Rates of convergence of internal and external iterative processes are used as a criterion of step changing. The solution convergence is estimated by the values of maximum stress and plastic strain. The technique developed in [16–18] is used to find the solution of approximate problem. The main difference from the technique incorporated for solving the rigorous problem lies in the absence of internal iterative process designed for the evolution equation integration [7]. There is only external iterative process for each time step [17].

6. Numerical results

There were two main aims of calculations performed. The first one is the determination of basic regularities of coupled thermomechanical processes in inhomogeneous viscoplastic bodies. The second one is the estimation of applicability of the approximate technique derived to solution of class of problems mentioned. The geometry of beam was chosen as follows: $a = 0.15 \text{ m}$, $b = 0.15 \cdot 10^{-1} \text{ m}$,

$b_1 = b_3 = 0.3 \cdot 10^{-2}$ m, $b_2 = 0.24 \cdot 10^{-1}$ m, where b_i , $i = 1, 2, 3$ are the layer thicknesses. Two possible configurations were studied. The first one has the composition aluminium-steel-aluminium (ASA) and the second one has the opposite SAS composition. The excitation frequency is 1Hz.

Comparison of results was performed for the following set of thermomechanical characteristics: 1) ranges of the equivalent stress and plastic strain $\sigma_{1,2}^a$, $\varepsilon_{1,2}^a$ at the points $x = 0.3 \cdot 10^{-1}$ m, $y = 0.146 \cdot 10^{-1}$ m (corresponds to subscript 1) and $x = 0.3 \cdot 10^{-1}$ m, $y = 0.1 \cdot 10^{-1}$ m (corresponds to subscript 2) that belong to the 1st and 2nd layers respectively; 2) the plastic power \bar{D}' averaged over the volume of the body; 3) the maximum over the period values of averaged over the volume stored energy \bar{W}_e and heating temperature the $\langle \theta \rangle$ at the point $x = 0.0$ m, $y = 0.15 \cdot 10^{-1}$ m. The expressions for these quantities for the rigorous model are given by

$$\begin{aligned} \left[\begin{array}{c} \sigma_{xxaN} \\ \varepsilon_{xxaN}^p \end{array} \right] &= \frac{1}{2} \left\{ \max_{T_N} \left[\begin{array}{c} \sigma_{xx}(t) \\ \varepsilon_{xx}^p(t) \end{array} \right] - \min_{T_N} \left[\begin{array}{c} \sigma_{xx}(t) \\ \varepsilon_{xx}^p(t) \end{array} \right] \right\}, \\ \bar{D}' &= \frac{1}{VT} \int_V \int_{(N-1)T}^{NT} \mathbf{s} : \dot{\varepsilon}^p dt dV, \\ \bar{W}_e &= \frac{1}{V} \max_{T_N} \int_V \left[\frac{1}{18K_V} (\text{tr } \boldsymbol{\sigma})^2 + \frac{1}{4G} \mathbf{s} : \mathbf{s} \right] dV. \end{aligned} \quad (37)$$

The same quantities in the case of approximate model should be calculated as follows:

$$\begin{aligned} \sigma_{xxaN} &= |\tilde{\sigma}_{xxN}|, \quad \varepsilon_{xxaN}^p = |\tilde{\varepsilon}_{xxN}^p|, \\ \bar{D}' &= \frac{\omega}{2V} \int_V \text{Im} (\tilde{\mathbf{s}}_N : \tilde{\varepsilon}_N^{p*}) dV, \\ \bar{W}_e &= \frac{1}{V} \int_V \left[\frac{1}{18K_V} (\text{tr } |\tilde{\boldsymbol{\sigma}}_N|)^2 + \frac{1}{4G} \tilde{\mathbf{s}}_N : \tilde{\mathbf{s}}_N^* \right] dV, \end{aligned} \quad (38)$$

where N denotes the number of cycle and complex conjugate is marked with asterisk.

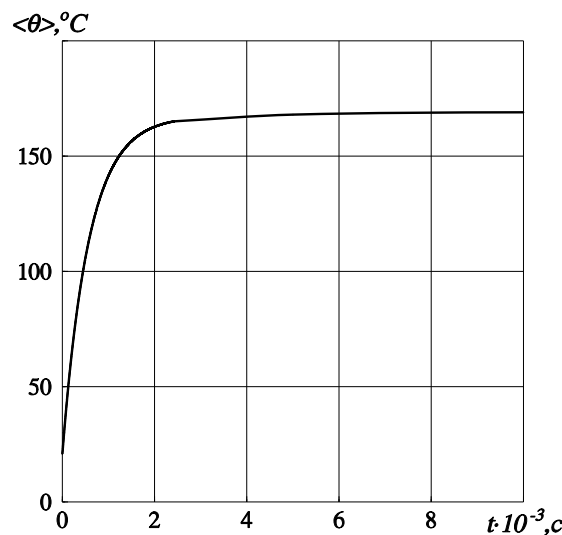


Fig. 3. Temperature evolution in time at the point with coordinates $x = 0.0$ m, $y = 0.15 \cdot 10^{-1}$ m.

Good agreement between two approaches should be emphasized. The following errors of the approximate solution were detected: 2% for stored energy, 3% for dissipated energy, 2% for equivalent

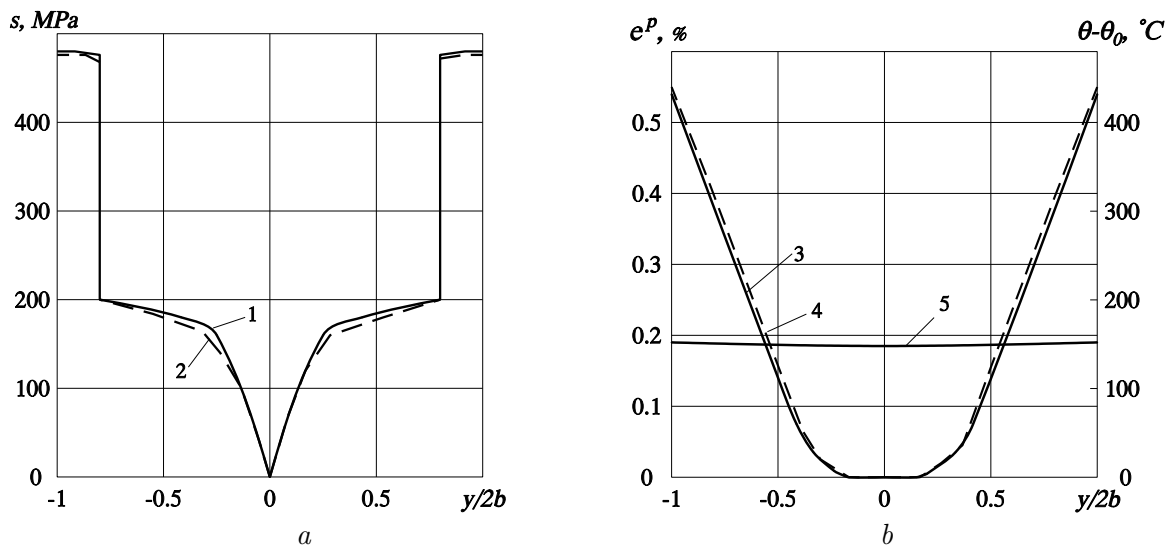


Fig. 4. Comparison of through the thickness distributions of the equivalent stress (a) and equivalent strain as well as steady temperature distribution over the cross-section $y = 0$ (b) provided by the complete and approximate problem statements for the ASA beam configuration.

stress, 8% for equivalent plastic strain and 3% for heating temperature at the stage of stabilized process. Maximum errors were detected at the starting cycles. They can be explained by larger errors in complex characteristics values at the beginning due to unclosed hysteresis loops.

Good agreement of the results mentioned provides possibility for approximate model application for investigation of the temperature evolution and stabilization process. The results of calculation are depicted in Fig. 3 for heat transfer coefficient $\gamma = 20 \text{ W/m}^2\text{K}$. Good agreement of results both in time and spatial coordinates should be emphasized.

Typical results of strain-stress state investigation for configurations ASA are shown in Fig. 4. The lines 1 and 2 depict equivalent stress range distribution over cross-section $y = 0$ for the complete and approximate problem statements respectively. Curves 3 and 4 have the same meaning for the equivalent plastic strain range distribution. They almost coincide for the chosen scale.

Good agreement between stored and dissipated energy values for complete and approximate problem statements provides a reason for applying the approximate technique to estimate the element damping properties. The following energy characteristics were considered for comparison of damping abilities of ASA and SAS beam compositions: \bar{D}' , \bar{W}_e and loss coefficient

$$\psi_L = \frac{2\pi \int_V \bar{D}'(\mathbf{x}) dV}{\omega \int_V \max_T \bar{W}(\mathbf{x}) dV}.$$

Results for the 7th cycle (steady vibrations regime) are presented in Tables 2 and 3. Indexes denote the number of layer.

Table 2. Energy characteristics of the beam-damper for the 7th cycle.

Composition	ψ_L	\bar{D}' , MPa/s	\bar{W}_e , MPa
ASA	5.04	4.65	0.922
SAS	8.02	4.76	0.593

Table 3. Energy characteristics of the damper layers for the 7th cycle.

Composition	$\psi_{L1,3}$	ψ_{L2}	$\bar{D}'_{1,3}$, MPa/s	\bar{D}'_2 , MPa/s	$\bar{W}_{e1,3}$, MPa	\bar{W}_{e2} , MPa
ASA	9.85	4.01	0.672	3.30	0.07	0.82
SAS	11.53	3.76	1.779	1.19	0.15	0.32

7. Conclusions

There is a good agreement between the solutions provided by the complete and approximate problem statements. The configuration SAS is characterized by a higher loss coefficient. It means that composition with thick enough internal layer of “soft” material covered by thin layers of a “hard” one is more suitable for damping of forced vibration for loading under consideration. Both complete and approximate models can be applied for solving the vibration and heat dissipation problem for inhomogeneous structures such as multi-layer beam-dampers. But it should be emphasized that in the case of harmonic loading, integration of the approximate statement demands two orders less time than the complete one.

-
- [1] Chiba T., Kobayashi N. Dynamic Characteristics of Pipe Systems Supported with Viscoelastic and Elasto-Plastic Dampers. *Trans. ASME, J. Appl. Mech.* **57**, 409 (1990).
 - [2] Shiba K., Mase S., Yabe Y., Tamura K. Active/passive vibration control systems for tall buildings. *Smart Mater. and Struct.* **7**, 588 (1998).
 - [3] Aizawa S., Kanizawa T., Higasino M. Case studies of smart materials for civil structures. *Smart Mater. and Struct.* **7**, 617 (1998).
 - [4] Lu L.-Y., Lin G.-L., Shih M.-H. An experimental study on a generalized Maxwell model for nonlinear viscoelastic dampers used in seismic isolation. *Eng. Struct.* **34**, 111 (2012).
 - [5] Bui H., Ehrlacher A., Nguyen Q. Thermomechanical coupling in fracture mechanics (in *Thermomechanical Couplings in Solids*. H.D. Bui and Q.S. Nguyen (Eds.) Elsevier; (1987).
 - [6] Kim D., Dargush G., Basaran C. A cyclic two-surface thermoplastic damage model with application to metallic plate dampers. *Eng. Struct.* **52**, 608 (2013).
 - [7] Zhuk Y., Senchenkov I. Investigation of energy characteristics of the layered beam-damper. *Jour. Comput. Appl. Mech.* **6**, 253 (2005).
 - [8] Senchenkov I., Zhuk Y. Resonance vibrations and dissipative heating of thin-walled laminated elements made of physically nonlinear materials. *Int. Appl. Mech.* **40**, 794 (2004).
 - [9] Irschik H., Ziegler F. Dynamic processes in structural thermoviscoplasticity. *Appl. Mech. Rev.* **48**, 301 (1995).
 - [10] Chan R., Lindholm U., Bodner S., Walker K. High Temperature Inelastic Deformation Under Uniaxial Loading: Theory and Experiment. *Trans. ASME, Jour. Eng. Mater. Technol.* **111**, 345 (1989).
 - [11] Bodner S. Lindenfeld A. Constitutive modeling of the stored energy of cold work under cyclic loading. *Eur. Jour. Mech., A / Solids.* **14**, 333 (1995).
 - [12] Bodner S. Partom Y. Constitutive equations for elastoviscoplastic strain hardening material. *Trans. ASME, Jour. Appl. Mech.* **42**, 385 (1975).
 - [13] Chaboche J.-L. Cyclic viscoplastic constitutive equations. Part 1: A thermodynamic consistent formulation. *Trans. ASME, Jour. Appl. Mech.* **60**, 813 (1993).
 - [14] Lubliner J. On the structure of the rate equations of materials with internal variables. *Acta Mechanica* **17**, 109 (1973).
 - [15] Senchenkov I., Zhuk Y. Thermoviscoplastic Deformation of Materials *Int. Appl. Mech.* **33**, 122 (1997).

- [16] Senchenkov I., Zhuk Y., Tabieva G. Thermodynamically consistent modification of generalized thermoviscoelastic models. *Int. Appl. Mech.* **34**, 53 (1998).
- [17] Zhuk Y., Senchenkov I. Approximate model of thermomechanically coupled inelastic strain cycling. *Int. Appl. Mech.* **39**, 300-306 (2003).
- [18] Senchenkov I., Zhuk Y., Karnaukhov V. Modeling the thermomechanical behavior of physically nonlinear materials under monoharmonic loading. *Int. Appl. Mech.* **40**, 943 (2004).
- [19] Zhuk Y., Chervinko O., Tabieva G. Planar flexural vibration and dissipative heating of laminated rectangular plates. *Int. Appl. Mech.* **38**, 837 (2002).
- [20] Zhuk Y., Guz I., Sands K. Monoharmonic approximation in the vibration analysis of a sandwich beam containing piezoelectric layers under mechanical or electrical loading. *J. Sound Vibr.* **330**, 4211 (2011).

Демпфіруючі характеристики тришарової балки-демпфера при гармонічному навантаженні

Жук Я. О.

*Київський національний університет імені Тараса Шевченка
вул. Володимирська, 64, 01601, Київ, Україна*

Досліджується термомеханічна поведінка неоднорідних в'язкопластичних елементів конструкцій при циклічному навантаженні на прикладі задачі про гармонічний згин та дисипативний розігрів тришарової балки. Використано дві постановки задачі. Одна ґрунтується на узагальненій термодинамічно узгодженій моделі непружної течії (повна постановка задачі), а інша формулюється з використанням наближеної склерономної моделі поведінки матеріалу (наближена постановка задачі). Алюмінієвий сплав та сталь вибрані в якості матеріалів шарів. Проведено порівняння результатів, отриманих в рамках повної та наближеної постановок. Дано порівняльну оцінку коефіцієнту втрат для різних конфігурацій балки.

Ключові слова: *термомеханічна зв'язаність, балка-демпфер, коефіцієнт втрат*

2000 MSC: 74, 74F, 74C, 74F05

УДК: 539.3